RSC Advances

PAPER

View Article Online
View Journal | View Issue

Cite this: *RSC Adv.*, 2024, **14**, 23621

A facile approach to fabricate a stabilized slippery lubricant-infused porous surface with dynamic omniphobicity for self-cleaning

Yingfen Huang

Received 22nd May 2024
Accepted 12th July 2024

DOI: 10.1039/d4ra03770g

rsc.li/rsc-advances

Developing a slippery lubricant-infused porous surface (SLIPS) is an important strategy for fabricating dynamically omniphobic surfaces. In this study, biocompatible and non-toxic liquid silicone rubber, TiO_2 nanoparticles, and dimethyl silicone oil were used to fabricate a SLIPS. Subsequently, systematic investigation was conducted to explore its associated properties and address existing challenges in this field. The chosen lubricant exhibited a strong chemical affinity towards the substrate, eliminating the need for any functionalization treatment prior to infusion. In addition, the fabricated SLIPS exhibited excellent dynamic omniphobicity as well as shear stability, thermal stability, chemical stability, and mechanical stability. Moreover, it demonstrated good self-cleaning performance for droplets, with varying surface energies, temperatures, and pH values, as well as for common dyes and contaminants. In addition, damage from external forces could self-repair on the SLIPS, which is beneficial for extending the service life and application range.

1 Introduction

Liquid droplets are ubiquitous, and the interaction between droplets and material surfaces affects all aspects of human life and social development, and thus they have received increasing attention. Antiwetting is a fundamental property in the contact between liquids and surfaces, and it can be investigated from two perspectives: static antiwetting, characterized by the contact angle (CA); and dynamic antiwetting, characterized by the sliding angle (SA) and contact angle hysteresis (CAH). It has been increasingly reported that the sole use of CA is inadequate to accurately represent the antiwetting behavior of material surfaces. Instead, it is more important to consider the dynamic antiwetting ability.[1–5] Therefore, the fabrication of surfaces with unique dynamic omniphobicity has gained rapid momentum in the advancement of new materials. Interestingly, it has shown broad application prospects in a variety of fields, including self-cleaning,[6–12] anti-fouling,[10–19] anti-corrosion,[8,16–21] drag reduction[14,21–23] and oil–water separation.[9,10,24–26]

Nepenthes is a representative dynamic omniphobic surface found in nature. Inspired by it, researchers have developed surfaces with dynamic omniphobicity that utilize a lubricant-infused structure.[20,27,28] This structure replaces the gases between pores with a liquid film of low surface energy and utilizes the microscopic roughness to trap the lubricant, creating a smooth, continuous solid–liquid composite interface, resulting in small SAs and CAHs. However, research on slippery lubricant-infused porous surfaces (SLIPSs) is still in the active exploration stage. There are various methods for fabricating a SLIPS; most of them involve three main steps: constructing a rough substrate, modifying and functionalizing the substrate (to ensure it has sufficient chemical affinity with the lubricant), and infusing the lubricant. Since repelled droplets are in direct contact with lubricants, the key to determining the properties of SLIPSs lies in the physicochemical properties of the lubricants. In order to achieve effective dynamic omniphobicity, most current SLIPSs use perfluoroalkanes or perfluoroethers as lubricants. To ensure chemical affinity between rough substrates and lubricants, the substrates must be initially treated with fluorine-containing compounds.[3,20,29–32] All of these factors make the preparation process complicated, expensive, and potentially polluting. Therefore, environmentally friendly, non-toxic methods utilizing low surface energy silicone oil or mineral oil have gained the attention of researchers.[33–35] In addition, improving the stability of SLIPS to achieve long-lasting omniphobicity is an urgent problem for practical applications.

In this study, a facile two-step approach was developed to fabricate a dynamically omniphobic SLIPS without modifying the substrate. A superhydrophobic porous rough substrate was first constructed using addition-cure liquid silicone rubber and TiO_2 nanoparticles. Then, dimethyl silicone oil as a lubricant was infused directly. The biocompatible raw materials are safe for both the human body and the environment. Hence, this SLIPS could be expected to have applications in the fields of medicine and food. The lubricant dimethyl silicone oil has a low surface energy and good chemical stability. It also exhibited

School of Pharmacy, Quanzhou Medical College, Quanzhou 362000, China. E-mail: yf_huang12345@163.com

good chemical affinity with the porous structure due to their common polydimethylsiloxane component. Therefore, there was no need to functionalize the structure before infusion, which resulted in a simpler process. Furthermore, the study systematically analyzed the shear stability, thermal stability, chemical stability, and mechanical stability of the SLIPS. On this basis, the self-repairing and self-cleaning performances were further investigated.

2 Experimental

Materials

Liquid silicone rubber Sylgard 184, titanium dioxide P25, and dimethyl silicone oil PMX-200 (100 mPa s) were purchased from Dow Corning, Degussa, and Aladdin, respectively. Hexamethylene, oleic acid, ethyl alcohol, hydrochloric acid, and sodium hydroxide were purchased from Sinopharm. Methylene blue, rhodamine, crystal violet, and acridine orange were purchased from Macklin. All the materials were used as received.

Preparation

1.10 g Sylgard 184 (with a weight ratio of A to B of 1 : 10) and 1.10 g P25 were added to 30 mL hexamethylene, then sealed in a glass bottle and fully dispersed using ultrasonic treatment and magnetic stirring. The mixture was dropped onto precleaned glass, and spin-coated at a speed of 300 rpm for 10 s followed by an increased speed of 800 rpm for 40 s. The hybrid porous surface was obtained after being cured at 125 °C for 55 min and was finally denoted as HPS.

Next, 50 μL PMX-200 was added onto the HPS and then spread spontaneously over the rough surface. After waiting for 2 min, the sample was spun at a speed of 2000 rpm for 40 s to remove excess dimethyl silicone oil. The slippery lubricant-infused porous surface was successfully fabricated and denoted as SLIPS. All the SLIPS samples were left to sit for 24 h before conducting any further experiments.

Characterization

The chemical compositions of HPS, dimethyl silicone oil and SLIPS, were analyzed using Fourier transform infrared spectroscopy in the attenuated total reflectance mode (ATR-FTIR, Thermo Nicolet 5700). The surface morphology of HPS was investigated by field emission scanning electron microscopy (FE-SEM, JEOL JSM-7500F). The measurements of distilled water and the oleic acid contact angle (CA), sliding angle (SA), and contact angle hysteresis (CAH) were carried out using a drop shape analyzer (KRUSS DSA 25) at room temperature. To measure the CA, a 2 μL probe droplet was gently placed on the surface of the horizontal sample, and the value was recorded once the reading stabilized. To measure the critical tilting angle SA, 30 μL distilled water or 15 μL oleic acid was dropped on the horizontal sample surface, then the program was started to rotate the sample stage until the probe droplet slid down. In this case, the contact angle in the forward direction of the droplet was θ_A, and the contact angle in the backward direction of droplet was θ_R, while the CAH was the difference between θ_A and θ_R. Each sample was measured three times at different locations, and the final value was calculated as the average of the three measurements.

3 Results and discussion

A slippery lubricant-infused porous surface (SLIPS) was prepared through a facile two-step approach. As shown in Fig. 1, the hybrid porous surface (HPS) was fabricated by compositing the addition-cure liquid silicone rubber Sylgard 184 and TiO_2 nanoparticles, and then the lubricant dimethyl silicone oil was directly infused without any functionalization treatment. Fig. 2a shows the ATR-FTIR spectra of HPS, dimethyl silicone oil, and SLIPS. For all the curves, the typical characteristic peaks of PDMS occurred at 1250 and 810 cm^{-1} due to the deformation vibration and stretching vibration of Si–CH_3, 1150 and 1020 cm^{-1} due to the stretching vibration of Si–O–Si, and 2900 and 1410 cm^{-1} due to the stretching vibration and deformation vibration of C–H. For the curve of HPS, the characteristic band occurred at 760 cm^{-1}, attributed to the stretching vibration of Ti–O. These results indicated that the hybrid surface HPS had formed and no chemical reaction had taken place between PDMS and TiO_2. Furthermore, the characteristic peaks of the SLIPS were essentially consistent with those of dimethyl silicone oil, indicating that the lubricant had successfully infused into the porous HPS and formed a lubricant film on its surface. In addition, no new chemical bonds were detected, so the lubricant and substrate HPS only interacted through intermolecular forces.

HPS exhibited superhydrophobicity (Fig. 3a), as indicated by its high contact angle (CA) of 153.17 ± 1.06° (greater than 150°), and low sliding angle (SA) 0.91 ± 0.19° and contact angle hysteresis (CAH) 4.35 ± 0.94° (both less than 10°), when in contact with water.[36] The FE-SEM images (Fig. 2b) revealed that a hierarchical micro/nanoporous structure was formed on HPS. The cooperative effect of the micro/nanoscale roughness and the low surface energy of PDMS modification on the nanoparticles contributed to its excellent water repellency, similar to that of lotus leaves. However, HPS lost its repellency for low surface energy liquids due to their enhanced ability to wet surfaces. Ethanol aqueous solutions with volume fractions ranging from 0–90% were prepared to simulate liquids spanning a wide range of surface energies. The solutions were stained with rhodamine for easy observation and self-cleaning testing. Then, 50 μL droplets were dropped onto HPS placed at 30°, and the antiwetting behaviors were observed and recorded, as shown in Fig. 4. At low ethanol concentrations, the droplets could roll off HPS smoothly. However, when the volume fraction increased to 30%, the droplet could not slide down. Instead, it adhered to the surface, leaving an obvious red stain after the droplet was removed. Similarly, water at 95 °C (stained with methylene blue) could adhere to and stain HPS due to the decrease in surface energy with the increase in temperature.

In order to address the limitations of HPS, dimethyl silicone oil as a lubricant was infused into HPS to fabricate

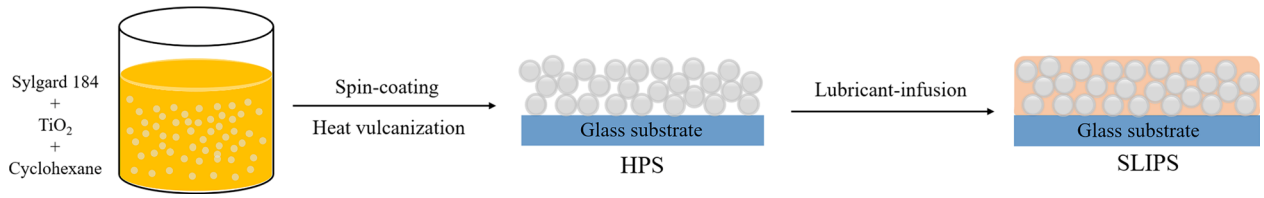

Fig. 1 Schematic for the preparation of the SLIPS.

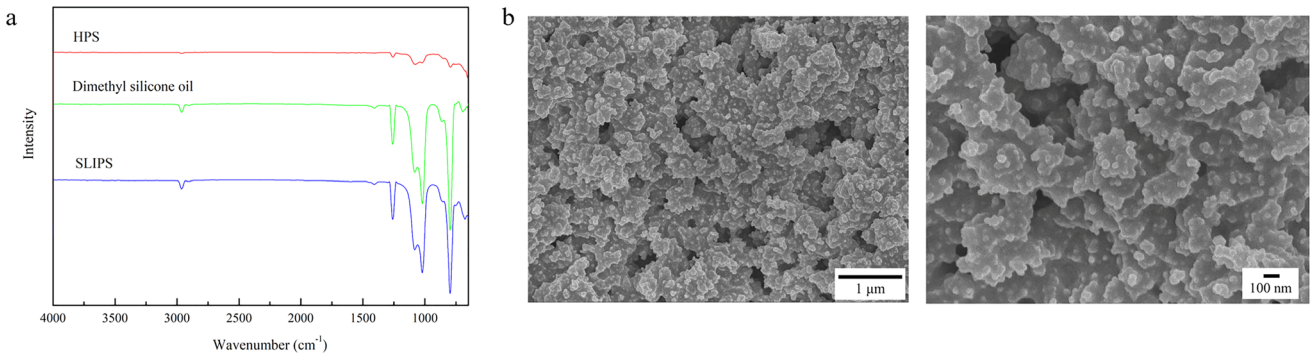

Fig. 2 (a) ATR-FTIR spectra of HPS, dimethyl silicone oil, and SLIPS. (b) FE-SEM images of HPS at the micrometer scale and nanoscale.

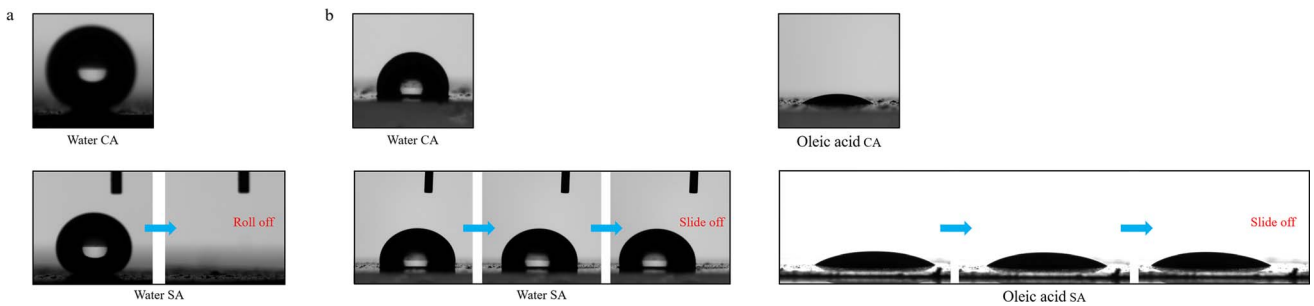

Fig. 3 (a) Superhydrophobicity of HPS. (b) Dynamic omniphobicity of the SLIPS.

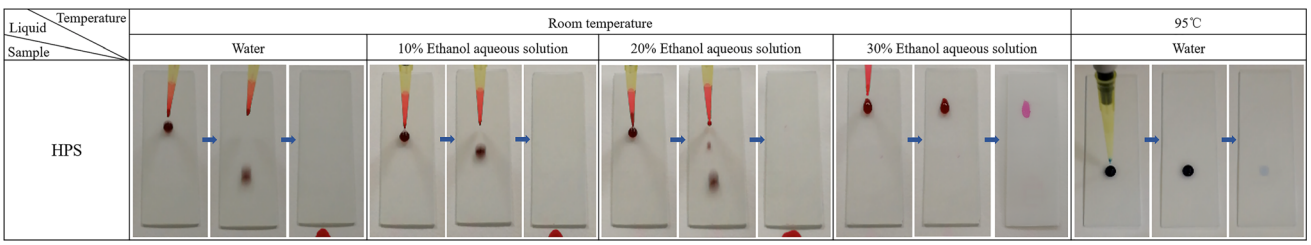

Fig. 4 Antiwetting behaviors of HPS toward ethanol aqueous solutions with varying volume fractions and water at different temperatures. (The size of the slides was 25.4 × 76.2 mm.)

a dynamically omniphobic SLIPS. Water and oleic acid were used to investigate the antiwetting properties of the SLIPS. The CA, SA, and CAH values of the water were 106.47 ± 0.91°, 1.64 ± 0.13°, and 1.96 ± 0.41°, while the values for oleic acid were 31.43 ± 0.70°, 2.11 ± 0.44°, and 4.65 ± 0.87°, respectively (Fig. 3b). Although the water and oleic acid CAs on the SLIPS were limited, they demonstrated excellent dynamic omniphobicity with SAs and CAHs all below 5°. The antiwetting behavior of the SLIPS was contributed by the thin lubricant film on the surface, not the micro/nanorough structure at the bottom.[37] However, the multiscale rough structure increased the contact area with the lubricant, providing enough space and capillary

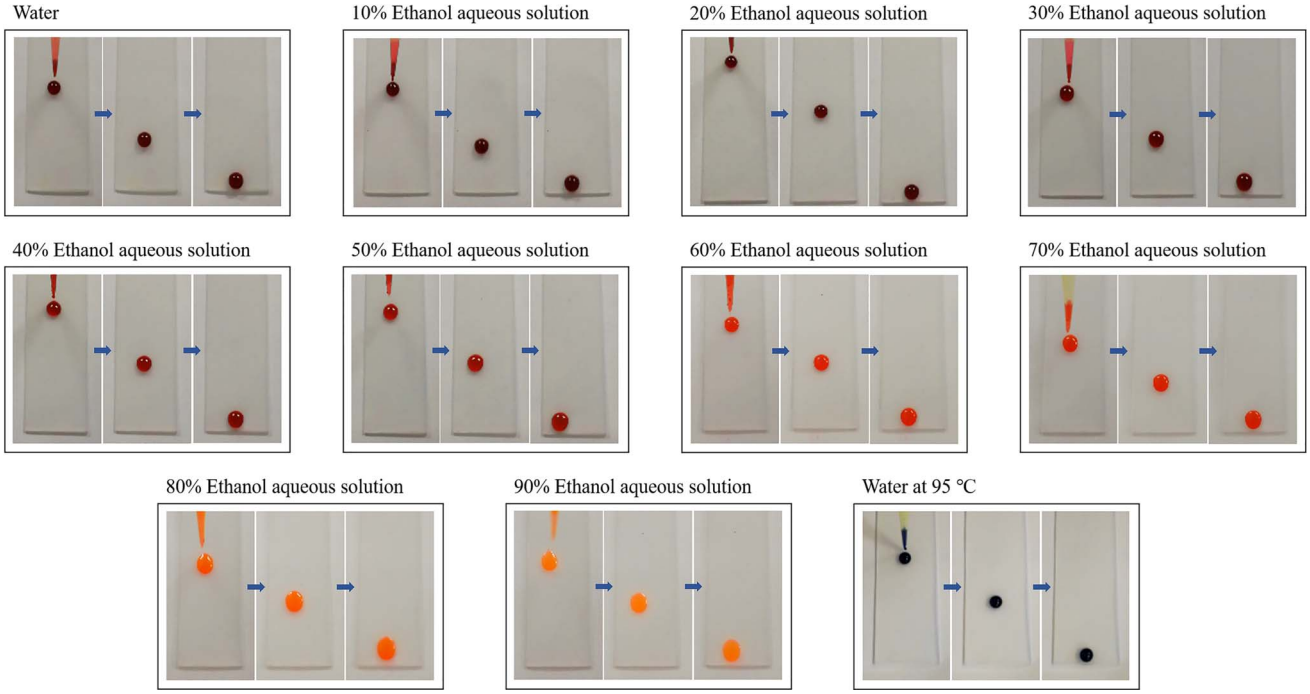

Fig. 5 Antiwetting properties of the SLIPS toward ethanol aqueous solutions with varying volume fractions and water at different temperatures. (The size of the slides was 25.4 × 76.2 mm.)

force to adsorb, retain, and lock the lubricant. The air in the pores of HPS was replaced with dimethyl silicone oil, resulting in a smooth, continuous, and chemically homogeneous interface on the SLIPS. The smoothness and uniformity of the lubricant film were conducive to effectively reducing sliding resistance, allowing the water and oleic acid to easily slide off. Furthermore, both the substrate liquid silicone rubber Sylgard 184 and the lubricant dimethyl silicone oil are polydimethylsiloxane, so they have good chemical affinity. The SLIPS was fabricated simply by directly infusing the lubricant without any additional functionalization treatment. Moreover, all the selected materials are biocompatible and safe for humans and the environment.

To further research the dynamic antiwetting of the SLIPS, 50 μL of ethanol aqueous solutions with varying volume fractions were dropped onto the SLIPS placed at 30°. As shown in Fig. 5, with the increase in ethanol concentration, the CA values gradually decreased, and the droplet shape changed from a sphere to a water-drop shape. However, the droplets with volume fractions ranging from 0–90% all slid off successfully, and no stains were left on the surface. In addition, water at 95 °C also slid off easily, and the surface

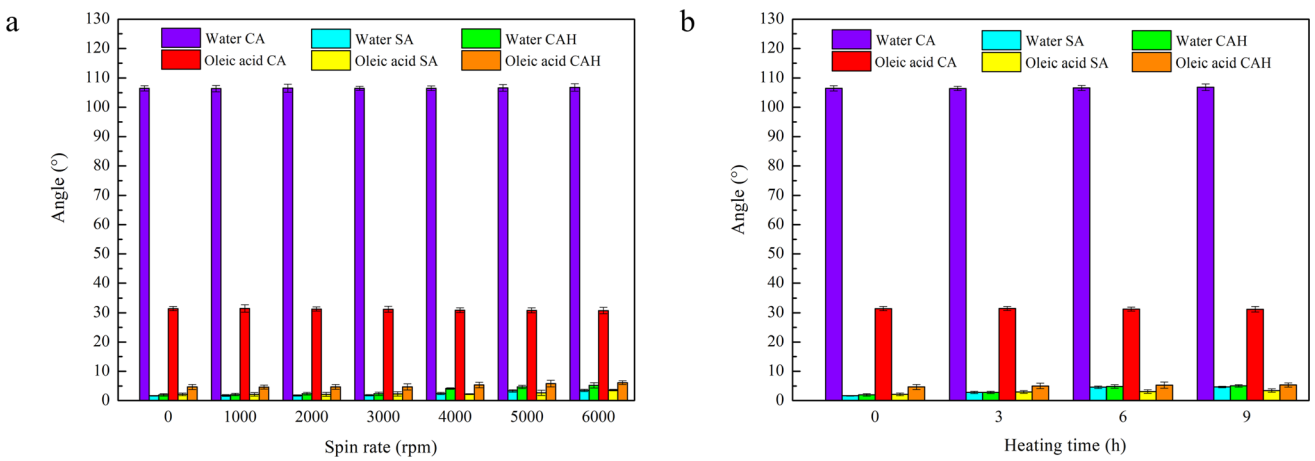

Fig. 6 Shear stability (a) and thermal stability (b) of the SLIPS.

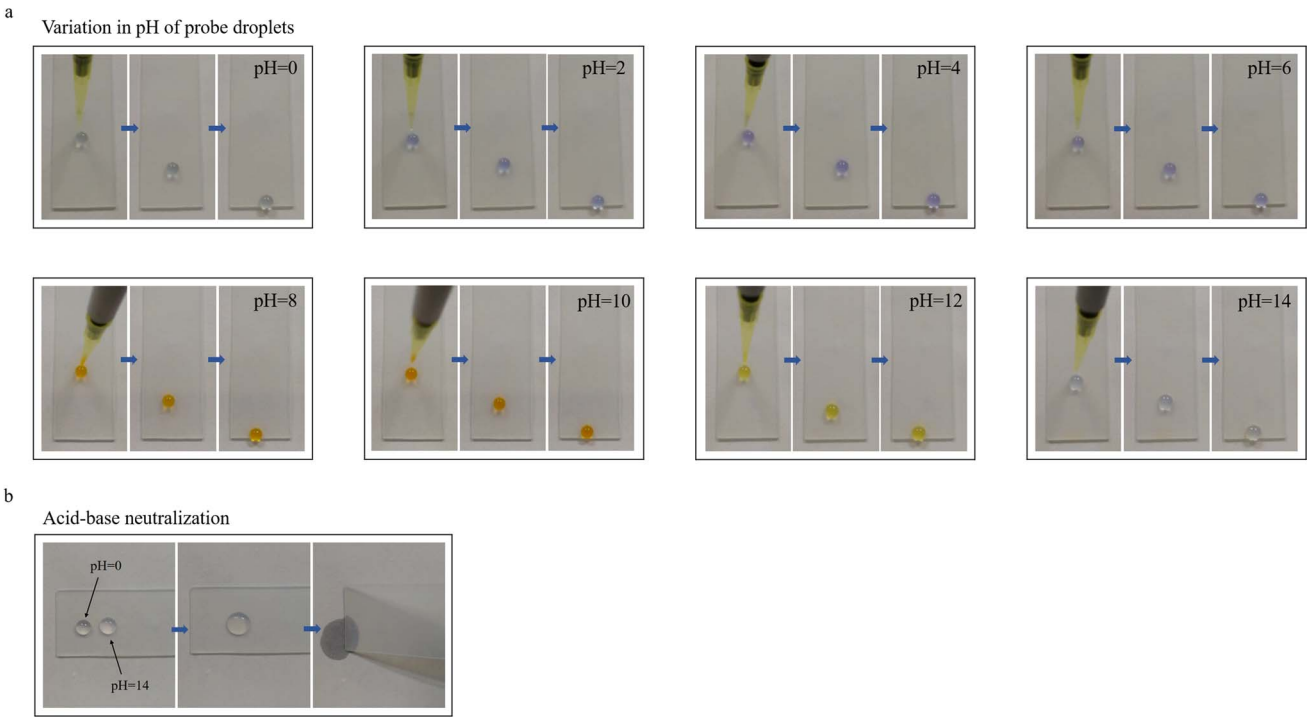

Fig. 7 Chemical stability tests, including varying the pH of the probe droplets (a) and conducting acid–base neutralization (b). (Acidic droplets were all stained with crystal violet, while alkaline droplets were all stained with acridine orange. The size of the slides was 25.4 × 76.2 mm.)

remained clean without any adhesion or trailing. It was demonstrated that the SLIPS exhibited excellent dynamic omniphobicity toward liquids with varying surface energies and temperatures.

Good stability is particularly important for practical applications. To investigate the shear stability, the SLIPS was fixed on a spin coater and rotated at speeds of 1000, 2000, 3000, 4000, 5000, or 6000 rpm for 1 min. Comparing the CA, SA, and CAH values of water and oleic acid on the rotated samples with the data from an unrotated SLIPS, the results are shown in Fig. 6a. The SLIPS basically maintained its antiwetting property under the action of shear force and exhibited good shear stability. The water and oleic acid CAs remained almost unchanged, and the SAs and CAHs remained very low. Even after being subjected to a shearing force of up to 6000 rpm, the SLIPS maintained excellent dynamic omniphobicity, as demonstrated by the water and oleic acid SAs of less than 4° and CAHs of less than 7°. The thermal stability experiments were carried out by placing the SLIPS samples in an oven at 200 °C and heating them for 3, 6, or 9 h. The measured data (Fig. 6b) showed that the CA, SA, and CAH values of water and oleic acid remained stable after heat treatment, indicating that the static and dynamic antiwetting properties were not significantly affected and the SLIPS exhibited excellent thermal stability.

Chemical stability is another crucial factor to consider in applications. In this study, three methods were adopted to examine the chemical stability of the SLIPS. First, 50 μL of acids or bases were dropped onto SLIPS placed at 30°, and the sliding behaviors of droplets were recorded, as shown in Fig. 7a. In order to enhance the visibility and examine the self-cleaning performance of the SLIPS toward different types of dyes, hydrochloric acid solutions were stained with crystal violet, while sodium hydroxide solutions were stained with acridine orange. Owing to the excellent chemical stability of the dimethyl silicone oil lubricant film on the SLIPS, all the acidic and alkaline droplets with varying pH values could slide off smoothly without leaving any traces or adhesion. Second, an acid–base neutralization reaction was performed on the SLIPS, as shown in Fig. 7b. Here, 50 μL of hydrochloric acid (pH = 0) and sodium hydroxide (pH = 14) droplets were separately applied onto the SLIPS. They were then combined and allowed to react. Subsequently, by gently lifting one end of the SLIPS, the reacted droplet slid off easily, leaving the surface clean and slippery. Third, the SLIPS samples were respectively soaked in hydrochloric acid (pH = 0) and sodium hydroxide (pH = 14) for 1 h, and then taken out and dried at 50 °C. The surfaces still retained good dynamic omniphobicity. The water CA, SA and oleic acid CA, SA of the SLIPS soaked in the acid were 107.43 ± 1.10°, 2.01 ± 0.33°, 31.16 ± 0.71°, 2.43 ± 0.54°, respectively, while the values were 107.76 ± 0.93°, 1.94 ± 0.28°, 30.88 ± 0.91°, 2.60 ± 0.67° for the sample soaked in the base. Thus, it could be demonstrated that the SLIPS had good chemical stability, and its dynamic omniphobicity was hardly affected by acidity, alkalinity, or acid–base reactions.

Surface structures are often damaged by external forces in real-life applications. For the micro/nanorough superhydrophobic surfaces that imitate lotus leaves, the damage is

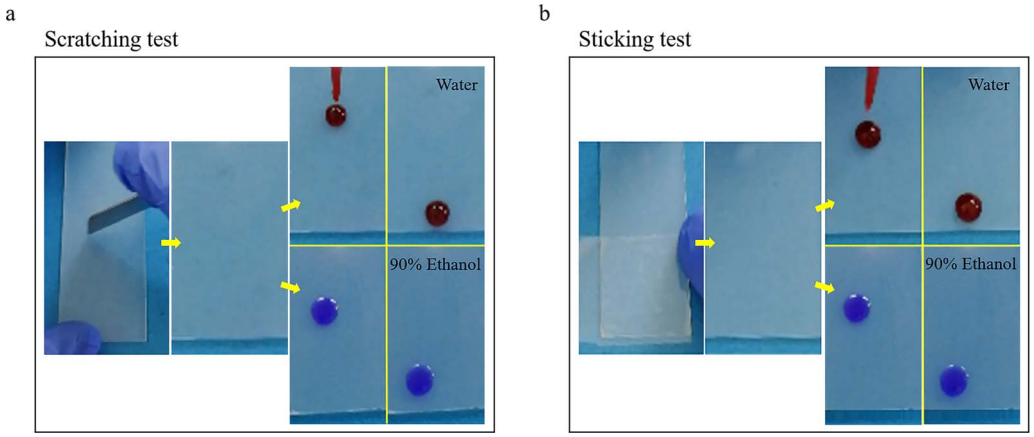

Fig. 8 Mechanical robustness tests included scratching with a knife (a) and sticking with tape (b). (The size of the slides was 25.4 × 76.2 mm.)

Table 1 Sliding speeds of water droplets on the SLIPS after the scratching or sticking tests

Number of tests	Sliding speed (scratching test) (mm s^{-1})	Sliding speed (sticking test) (mm s^{-1})
0	27.19 ± 0.03	27.19 ± 0.03
2	27.13 ± 0.06	27.18 ± 0.02
4	27.01 ± 0.07	26.63 ± 0.11
6	26.94 ± 0.17	26.33 ± 0.09

irreversible, and the surfaces may lose some or even all of their hydrophobic properties. Therefore, a mechanically robust antiwetting surface or a surface with self-repairing capability is urgently needed. Herein, the mechanical robustness of the SLIPS was tested by scratching with a knife and sticking with tape. Fig. 8a shows multiple scratching processes on the SLIPS, while the application of a large area external force using sticking tape was further investigated in Fig. 8b. There was no visible damage on the surface, and droplets of water (stained with rhodamine) and 90% ethanol (stained with crystal violet) both slid smoothly across the treated scope placed at 30° without leaving any stains. A significant amount of dimethyl silicone oil was stored in the micro/nanoporous structure of HPS. When the SLIPSs were subjected to external damage, the lubricant stored in nearby pores could spontaneously and promptly redistribute to fill the damaged area, helping maintain the smoothness and uniformity of surfaces, achieve the self-repairing function, and attain an indestructible dynamic omniphobicity. Quantitative characterization experiments for the scratching and sticking tests were further conducted. The experiments measured the sliding speeds of 50 μL water droplets on the SLIPS placed at 30° after 2, 4, and 6 scratching or sticking tests, and the results were recorded, and are compiled and detailed in Table 1.

Owing to the smoothness, homogeneity, and low surface energy of the lubricant film on its surface, the SLIPS exhibited excellent dynamic omniphobicity, effectively preventing liquid penetration or adhesion. Liquids with varying surface energies or pH values, stained with different types of dyes, could be easily removed from the SLIPS with minimal shear force, demonstrating the potential for self-cleaning. Seven common contaminants in daily life were selected to test the self-cleaning performance of the SLIPS, including orange juice, cola, coffee, green tea, milk, vinegar, and soy sauce (Fig. 9). All the droplets of the contaminants slid completely down from the SLIPS fixed on a stage tilted to 30°, without any adhesion, trailing, or staining. The excellent self-cleaning performance can enable the SLIPS to have a wide range of application prospects.

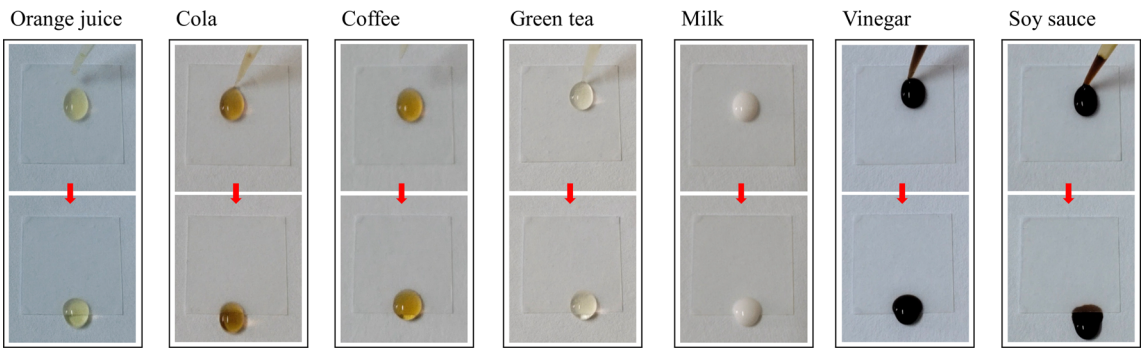

Fig. 9 Self-cleaning performance of the SLIPS. (The size of the coverglass was 20 × 20 mm.)

4 Conclusions

In summary, a dynamically omniphobic SLIPS was successfully fabricated by directly infusing the lubricant dimethyl silicone oil into a rough porous HPS that was prepared using liquid silicone rubber and TiO_2 nanoparticles. The SA values of water and oleic acid on the SLIPS were as low as $1.64 \pm 0.13°$ and $2.11 \pm 0.44°$, respectively. By replacing the air within the pores with a lubricant film, the SLIPS had a smooth, continuous, and chemically uniform surface, effectively reducing sliding resistance. Therefore, the SLIPS exhibited excellent dynamic omniphobicity and self-cleaning performance when exposed to droplets with varying surface energies, temperatures, pH values, as well as to common dyes and contaminants. The SLIPS also demonstrated exceptional shear, thermal, chemical, and mechanical stability through a series of experiments. Moreover, the SLIPS could realize self-repairing when subjected to external damage. Because of having the same chemical component polydimethylsiloxane, the lubricant and substrate had good chemical affinity. Therefore, this approach was facile and did not require any additional functionalization treatment. The materials selected for this study were all biocompatible and non-toxic to both humans and the environment. It is believed that the SLIPS has promising applications in medicine, food processing, marine antifouling, and other fields.

Data availability

The data supporting the findings of this study are available within the article.

Conflicts of interest

There are no conflicts to declare.

Acknowledgements

This work was supported by the Science and Technology Bureau of Quanzhou (grant number 2021N126S).

References

1 Q. Zhu, B. Li, S. Li, G. Luo, B. Zheng and J. Zhang, *J. Colloid Interface Sci.*, 2020, **578**, 262–272.
2 Z. Yin, F. Yuan, D. Zhou, M. Xue, Y. Luo, Z. Hong and C. Xie, *Chem. Phys. Lett.*, 2021, **771**, 138558.
3 B. Li and K. Li, *Appl. Surf. Sci.*, 2022, **598**, 153782.
4 M. Blosi, F. Veronesi, G. Boveri, G. Guarini and M. Raimondo, *Surf. Coat. Technol.*, 2021, **421**, 127419.
5 J. Wei, B. Li, N. Tian, J. Zhang, W. Liang and J. Zhang, *Adv. Funct. Mater.*, 2022, **32**, 2206014.
6 Y. Cao, A. Salvini and M. Camaiti, *J. Colloid Interface Sci.*, 2021, **591**, 239–252.
7 B. Chen, Z. Dong, Y. Jia, J. Li, M. Zhang and K. Zhang, *Prog. Org. Coat.*, 2021, **157**, 106297.
8 B. Zhang, J. Yan, X. Li and B. Hou, *J. Mater. Res. Technol.*, 2023, **23**, 1094–1104.
9 S. Pal, S. Mondal, P. Pal, A. Das, S. Pramanik and J. Maity, *Colloid Interface Sci. Commun.*, 2021, **44**, 100469.
10 P. Esmaeilzadeh, M. H. Ghazanfari and A. M. Dehkordi, *Ind. Eng. Chem. Res.*, 2022, **61**, 8005–8019.
11 B. Li, W. Liang, B. Zhang and J. Zhang, *Colloids Surf., A*, 2023, **672**, 131759.
12 W. Si, J. Wu and Z. Guo, *New J. Chem.*, 2023, **47**, 9989–9993.
13 H. Zhao, S. Khodakarami, C. A. Deshpande, J. Ma, Q. Wu, S. Sett and N. Miljkovic, *ACS Appl. Mater. Interfaces*, 2021, **13**, 38666–38679.
14 M. Yu, M. Liu, D. Zhang and S. Fu, *Chem. Eng. J.*, 2021, **422**, 130113.
15 G. Yang, Z. Zhang, C. Li and J. Hu, *Prog. Org. Coat.*, 2023, **179**, 107488.
16 C. Guo, H. Ding, M. Xie, H. Zhang, X. Hong, L. Sun and F. Ding, *Colloids Surf., A*, 2021, **615**, 126155.
17 X. Li, Q. Wang, L. Lei, Z. Shi and M. Zhang, *Constr. Build. Mater.*, 2021, **299**, 123945.
18 Z. Qiao, G. Ren, X. Chen, Y. Gao, Y. Tuo and C. Lu, *ACS Omega*, 2023, **8**, 804–818.
19 X. Gu, H. Jiang, X. Chen, Y. Li and G. Wang, *E-Polymers*, 2023, **23**, 20230116.
20 M. Zhang, J. Yu and J. Wang, *Surf. Coat. Technol.*, 2021, **407**, 126772.
21 M. Fakhri, B. Rezaee, H. Pakzad and A. Moosavi, *Tribol. Int.*, 2023, **178**, 108091.
22 P. Pathak and H. S. Grewal, *Colloids Surf., A*, 2023, **658**, 130675.
23 J. Su, F. Su, H. Yu, Z. Lin and J. Sun, *Appl. Surf. Sci.*, 2023, **634**, 157644.
24 M. Xia, X. Yi, S. Pan, Y. Liu, H. Li, Z. Sun, X. Jiang and Y. Zhang, *Mater. Chem. Phys.*, 2022, **276**, 125447.
25 T. Chen, S. Feng, X. Shen, F. Zhang, Z. Zhong, H. Wu and W. Xing, *Sep. Purif. Technol.*, 2023, **322**, 124217.
26 L. Jing, P. Yang, X. Lu, H. Tian, J. Mao, J. Li, F. Ma and Z. Zhang, *Appl. Surf. Sci.*, 2023, **608**, 155125.
27 L. Jiao, J. Tong, Y. Wu, Y. Hu, H. Wu, D. Li and R. Chen, *Appl. Surf. Sci.*, 2022, **576**, 151684.
28 W. Liu, R. Pan, M. Cai, X. Luo, C. Chen, G. Jiang, X. Hu, H. Zhang and M. Zhong, *J. Mater. Chem. A*, 2020, **8**, 6647–6660.
29 X. Han, W. Dou, S. Chen, S. Zhu, Y. Pu, H. Li, W. Wang and W. Li, *Surf. Coat. Technol.*, 2020, **388**, 125596.
30 Z. Chen, Y. Lu, R. Li, R. J. Orlando, R. Manica and Q. Liu, *Chem. Eng. J.*, 2022, **439**, 135688.
31 B. Zhang, W. Xu, Q. Zhu, F. Guan and Y. Zhang, *J. Ind. Eng. Chem.*, 2022, **107**, 259–267.
32 Y. Xiao, J. Huang and Z. Guo, *Mater. Chem. Phys.*, 2023, **307**, 128199.
33 S. Sahoo and R. Mukherjee, *Colloids Surf., A*, 2023, **657**, 130514.

34 L. Qin, H. Yang, F. J. Mawignon, Y. Zhang and G. Dong, *Prog. Org. Coat.*, 2023, **174**, 107275.
35 Y. Wei, Y. Yu, Y. Wang, Y. Jing, H. Gao, B. Li, S. Hu, R. Qiu, Y. Ouyang and G. Huang, *J. Coat. Technol. Res.*, 2023, **20**, 647–660.
36 T. Walter, T. Hein, M. Weichselgartner, K. Wommer, M. Aust and N. Vogel, *Green Chem.*, 2022, **24**, 3009–3016.
37 J. D. Smith, R. Dhiman, S. Anand, E. Reza-Garduno, R. E. Cohen, G. H. McKinley and K. K. Varanasi, *Soft Matter*, 2013, **9**, 1772–1780.